Journal of Structural Chemistry. Vol. 59, No. 3, pp. 520-528, 2018.

FIRST-PRINCIPLES STUDY OF THE STRUCTURES AND ELECTRONIC PROPERTIES OF $Ni_{n-1}Al$ (n = 2-20) CLUSTERS

W. Song[1], B. Wang[1], H.-Q. Li[3], J.-L. Wang[1], and C.-Z. He[2]

The electronic properties, such as binding energy, magnetic property, charge transfer, ionization potential, and electron affinity, of $Ni_{n-1}Al$ (n = 2-20) neutral and ionic clusters are studied using the density functional theory calculations with the PBE exchange-correlation energy functional. The calculated total magnetic moments and ionization potential can decrease and increase with the addition of the Al atom, respectively. The calculated electron affinity has occurred with no significant change, except the $Ni_{16}Al$ cluster.

DOI: 10.1134/S0022476618030046

Keywords: magnetic property, charge transfer, ionization potential, electron affinity.

INTRODUCTION

Atomic clusters have attracted attention and are still a matter of intense research because of their unique combination of molecular and condensed matter physics. Of particular interest are the binary clusters which may vary with the composition and atomic ordering, as well as the size of the clusters [1-3]. Nickel clusters have been widespread concerned because of their extensive catalytic and important magnetic properties. Aluminum is used as a conductor in electronic devices. Hence, the nickel-aluminum alloys and, in general, nickel-based superalloys have attracted much attention because of their wide applications in advanced material technology. In recent years, a number of studies have discussed the structures and electronic properties of Ni–Al alloy clusters [4-9]. Wen et al. calculated the energetically global minimum geometries and electronic states of Ni_nAl (n = 2-8) neutral clusters using the density functional theory with the generalized gradient approximation (GGA) for the exchange-correlation potential [4]. They also investigated various structural possibilities for binary alloy Ni_nAl^+ (n = 1-8) cationic isomers using the density functional method (BPW91) with the effective core potential LanL2DZ basis set [5]. The investigation of the structures, stabilities, and magnetism of Ni_mAl_n (m = 1-3, n = 1-9) clusters has been made by Zhang et al. They found that the mixed species preferred to adopt three-dimensional (3D) structures starting from four atoms and some charges transferred from Al to Ni atoms using the Mulliken population analysis [6]. Deshpande et al. reported the magnetic properties of small $Ni_{13-n}Al_n$ clusters with n = 0-13 calculated in the framework of the density functional theory. The cluster magnetic moment decreases with the sequential Al substitution for Ni atoms, which can be attributed to a greater degree of hybridization that forces the pairing of electrons in the Ni and Al molecular orbitals [7]. Shah et al. investigated the equilibrium structure, electronic, and magnetic properties of $Ni_{3n}Al_n$ (n = 1, 8) clusters using *ab*

[1]Physics and Electronic Engineering Department, Xinxiang University, Xinxiang, P. R. China. [2]Physics and Electronic Engineering College, Nanyang Normal University, Nanyang, P. R. China; hecz2013@nynu.edu.cn. [3]School of International Education and Exchange, Xinxiang University, Xinxiang, P. R. China. The text was submitted by the authors in English. *Zhurnal Strukturnoi Khimii*, Vol. 59, No. 3, pp. 544-552, March-April, 2018. Original article submitted September 11, 2016.

initio total-energy calculations based on the density functional theory. They found the magnetic moment per atom in these clusters to be significantly enhanced with respect to the bulk and a net charge transfer from the Ni *d*-type orbital to the Al *p*-type orbital [8]. The geometric structures and electronic properties of Al_mNi_n (m+n = 2-4) microclusters were investigated using a hybrid density-functional method (B3PW91) within the effective core potential by Hao et al. [9] and so on.

Although the investigations of Ni–Al clusters mentioned above have been performed, our knowledge about the properties of the Ni–Al clusters and the alloy cluster ions with a number of more than 8 is still limited. Therefore in this study, we have investigated the $Ni_{n-1}Al$ (n = 2-20) alloy clusters theoretically by applying the DFT method implemented in the Vienna *ab initio* Simulation Package (VASP). Based on the neutral and ionic Ni–Al alloy cluster structures optimized from our DFT-PBE calculations, the magnetic moment, binding energy, charge transfer, ionization potential, and electron affinity of the clusters have been systematically analyzed as the cluster size increases, which can provide useful information for the stabilities and properties of Ni–Al alloy clusters in this range. The purpose of this study is to provide the fundamental data for the future estimation of the magnetic alloy materials.

COMPUTATIONAL METHODS

The lowest-energy structures of neutral and ionic Ni_n (n = 2-20) clusters derived from [10-14] were verified using density functional theory (DFT) calculations. According to the lowest-energy structures of the nickel clusters, the most stable structures of neutral and ionic $Ni_{n-1}Al$ (n = 2-20) clusters have been obtained. DFT has evolved into a widely applicable computational technique, while requiring less computational effort than convergent quantum mechanical methods such as the coupled cluster theory. Our calculations were carried out using VASP [15, 16]. GGA with the Perdew, Burke, and Ernzerhof (PBE) function was used to deal with the exchange-correlation energies and the projected augmented wave (PAW) pseudopotential method was used to describe the electron-ion interactions. The Monkhorst-Pack 1×1×1 *K*-point mesh was used to sample Brillouin zone integration. The cutoff energy of plane waves in the calculations was taken to be 269.5 eV. A simple cubic supercell of a size of 20 Å was used. The geometry optimization of each isomer was carried out until the energy was converged to an accuracy of 10^{-5} eV.

RESULTS AND DISCUSSION

Structures of the neutral and ionic Ni_n (n = 2-20) clusters. Using the first-principles DFT-PBE calculations, the lowest-energy structures of the neutral Ni_n (n = 2-20) clusters were displayed in Fig. 1 [14]. The stable Ni_{3-6} structures are the triangle, tetrahedron, tetragonal pyramid, and square bipyramid (or octahedron), respectively. The Ni_{7-9} structures are formed by capping one, two, or three atoms to the Ni_6 octahedron structure. The Ni_{10} and Ni_{11} structures are a tetrahedron and a tetra-capped pentagonal bipyramid, respectively. It is well accepted that the Ni_{13} ground-state structure is a perfect icosahedron. The Ni_{12} structure is viewed as removing a Ni atom from the Ni_{13} surface. For Ni_{14} to Ni_{18}, the growth pattern is mainly based on the mechanism of capping extra atoms on the Ni_{13} icosahedron. The lowest-energy Ni_{14} structure is a capped icosahedron on one of its faces; those of $Ni_{15,16}$ are the adjacently bicapped icosahedron and a tricapped icosahedron. The Ni_{17} structure consists of four adjacently capped atoms on an icosahedron; Ni_{18} is formed by capping one more atom to Ni_{17}. The Ni_{19} structure, which is a perfect double-interpenetrating icosahedron, undergoes a transition, and Ni_{20} can be viewed as adding one atom to the side face in the waist of Ni_{19}. It has been found that the lowest-energy structures of the cluster anions were almost identical with the neutral ones. For cluster cations, only the Ni_5^+ structure is different from the neutral one (Fig. 3). The Ni_5^+ structure is a trigonal bipyramid.

Structures of the neutral and ionic $Ni_{n-1}Al$ (n = 2-20) alloy clusters. In this section, we have discussed the structures of $Ni_{n-1}Al$ (n = 2-20) clusters. The lowest-energy structures of $Ni_{n-1}Al$ (n = 2-20) clusters are presented in Fig. 2. All Ni atoms of Ni_{2-4} and Ni_6 are equivalent, so the NiAl, $Ni_{2-3}Al$ and Ni_5Al structures are viewed as an Al atom substitution

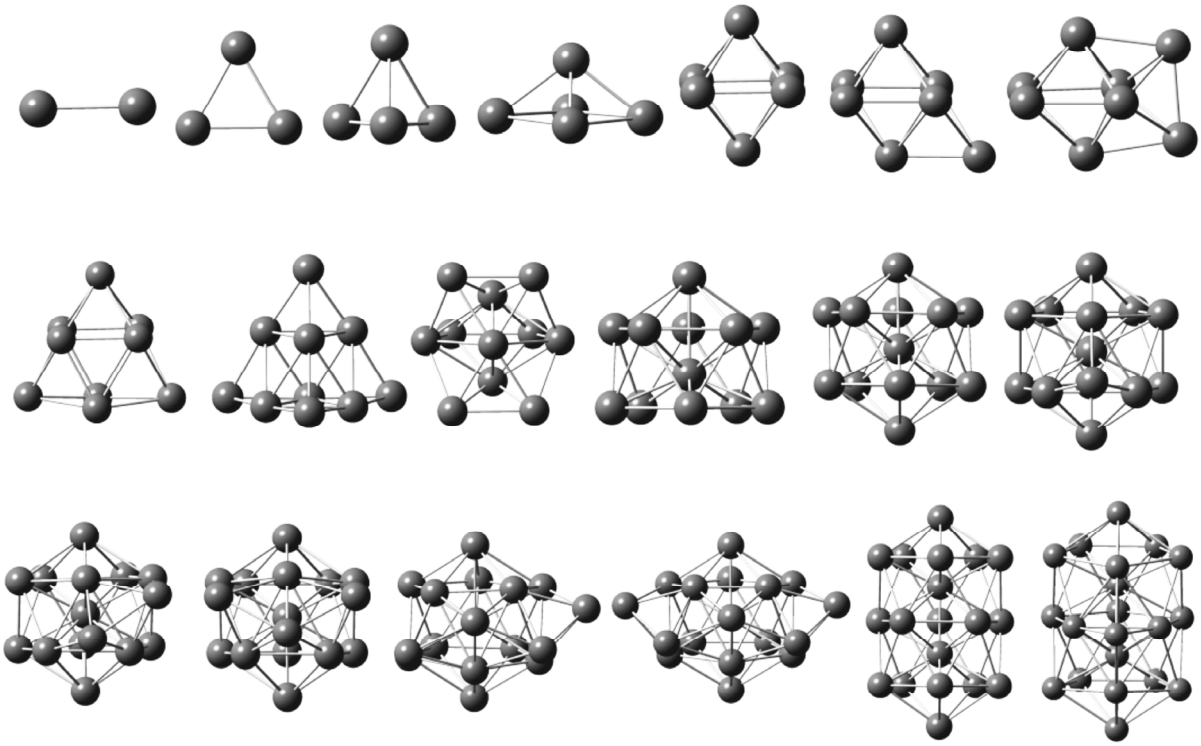

Fig. 1. Lowest-energy structures of the Ni_n (n = 2-20) clusters calculated at the DFT-PBE level.

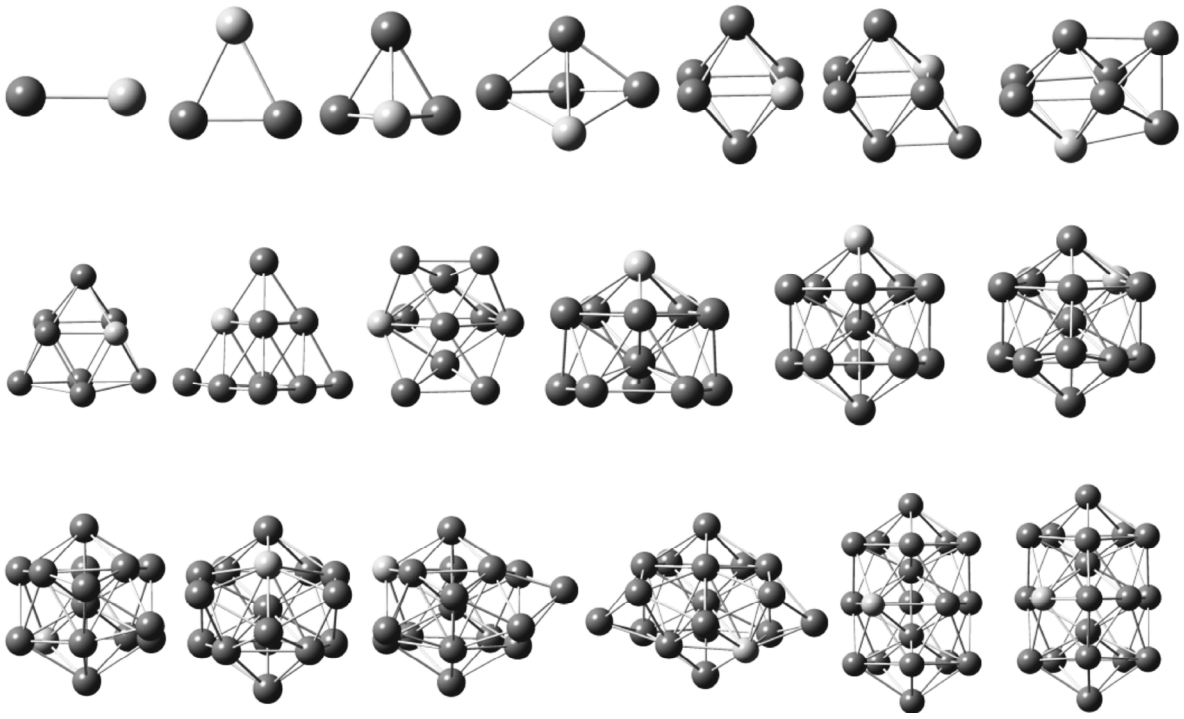

Fig. 2. Lowest-energy structures of the $Ni_{n-1}Al$ (n = 2-20) clusters calculated at the DFT-PBE level.

for any Ni atom. The Ni_4Al, Ni_6Al, and Ni_8Al structures can be obtained by an Al atom substitution for any Ni atom on the square. However, for Ni_7Al and $Ni_{11}Al$, it is obvious that the Al atom is preferable for the vertex site. The Ni_{10} and Ni_{11} structures are a tetrahedron and a tetra-capped pentagonal bipyramid, respectively. The Ni_9Al and $Ni_{10}Al$ structures are found to be an Al atom located at any site of the middle layer. From our present study the energetically most favorable $Ni_{12}Al$

structure can be viewed as an Al atom substitution for a Ni atom on the Ni_{13} surface site. The $Ni_{13\text{-}17}Al$ structures can be obtained by an Al atom substitution for the surface Ni atom of the icosahedron. For $Ni_{18\text{-}19}Al$, the structures are formed by an Al atom replacing one of the waist Ni atoms in Ni_{19} and Ni_{20}, respectively.

The ionic structures similar to the neutral structures are not repeated in Fig. 2. The structures of $Ni_{10}Al^-$, $Ni_{12}Al^+$, $Ni_{14}Al^+$, $Ni_{18}Al^+$ and $Ni_{19}Al^+$ clusters are shown in Fig. 3 because the Al atom has a different doped site compared with their neutral. The $Ni_{10}Al^-$ structure is viewed as an Al atom substitution for a Ni atom in the bottom layer. The $Ni_{12}Al^+$ structure is found to be an Al atom located at the central site. Compared to $Ni_{14}Al$ and $Ni_{19}Al$, the $Ni_{14}Al^+$ and $Ni_{19}Al^+$ structures are formed by an Al atom replacing another surface Ni atom. The $Ni_{18}Al^+$ structure is preferable to the Al-centered configuration.

Relative stabilities. In order to understand the relative stability of the $Ni_{n-1}Al$ (n = 2-20) clusters, we have analyzed the binding energy (E_b) and second energy differences (Δ_2E) for $Ni_{n-1}Al$ compared to Ni_n. The calculated results are shown in Fig. 4*a* and *d*. E_b of Ni_n and $Ni_{n-1}Al$ clusters are calculated according to the following definition:

$$E_b(Ni_n) = [nE(Ni) - E_{tot}(Ni_n)]/n,$$

$$E_b(Ni_{n-1}Al) = [(n-1)E(Ni) + E(Al) - E_{tot}(Ni_{n-1}Al)]/n,$$

where $E_{tot}(Ni_n)$ and $E_{tot}(Ni_{n-1}Al)$ are the total energies of Ni_n and $Ni_{n-1}Al$ clusters. E(Ni) and E(Al) are the energies of free Ni and Al atoms, respectively. By this definition, the larger the E_b value, the more stable the cluster is. It is found from observing Fig. 4*a* that the binding energy of $Ni_{n-1}Al$ clusters increases monotonically as a function of the cluster size. This curve has the same trend as the binding energy/atom for pure Ni_n clusters. This remarkable similarity is because of the similar geometrical structures with an Al atom substitution for a Ni atom for $Ni_{n-1}Al$ clusters.

The relative stability of the clusters can also be estimated through the second energy difference that is defined as $\Delta_2E(n) = E(n+1) + E(n-1) - 2E(n)$, in which $E(n)$ represents the total energy of the cluster of a size n. According to this definition, the clusters with positive Δ_2E are more stable than those with negative Δ_2E. The second energy difference is a sensitive quantity that can reflect the relative stability of the clusters and can be directly compared with the experimental relative abundance. Calculated Δ_2E for the Ni_n and $Ni_{n-1}Al$ clusters are plotted in Fig. 4*d*, showing an oscillating behavior. $Ni_{n-1}Al$ at n = 6, 8, 10, 11, 13, and 18 correspond to the local maxima on the Δ_2E curve, indicating that they are relatively more stable than the others.

We have also calculated and analyzed the binding energy per atom E_b (ion) and the second energy difference Δ_2E (ion) for the cationic and anionic clusters, as shown in Fig. 4*b-c* and *e-f*, respectively. According to the energy analysis, there are several peaks at n = 3, 6, 10, and 16 for the $Ni_{n-1}Al^+$ clusters, and at n = 5, 6, 8, 11, and 17 for the $Ni_{n-1}Al^-$ clusters, showing that these cluster ions are relatively more stable.

Magnetic properties. Nickel clusters are typically ferromagnetic 3*d* transition metal clusters. The Ni atom configuration is $3d^84s^2$. The electron spin follows the Pauli exclusion principle and the Hund rules, and two unpaired 3*d* electrons of the Ni atom contribute to its magnetic property. In principle, both spin and orbital magnetic moments have contributions to the total magnetic moment in any system. The orbital magnetic moment can be produced by the orbital motion of each electron while the spin magnetic moment can be produced by electron spin. The recent experiments found that the orbital moments could be as large as 10% to 30% of the spin moment [17]. Therefore, for the 3*d* transition metals, the

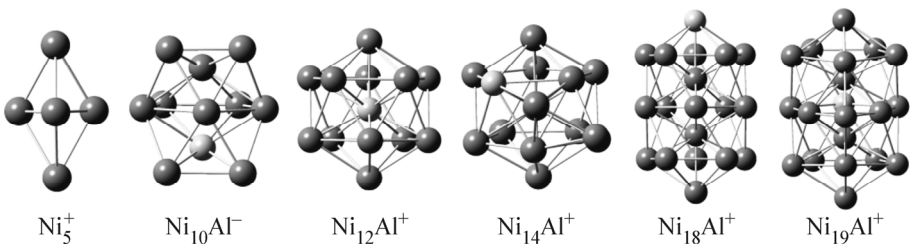

Fig. 3. Lowest-energy structures of Ni_5^+, $Ni_{10}Al^-$, $Ni_{12}Al^+$, $Ni_{14}Al^+$, $Ni_{18}Al^+$, and $Ni_{19}Al^+$ calculated at the DFT-PBE level.

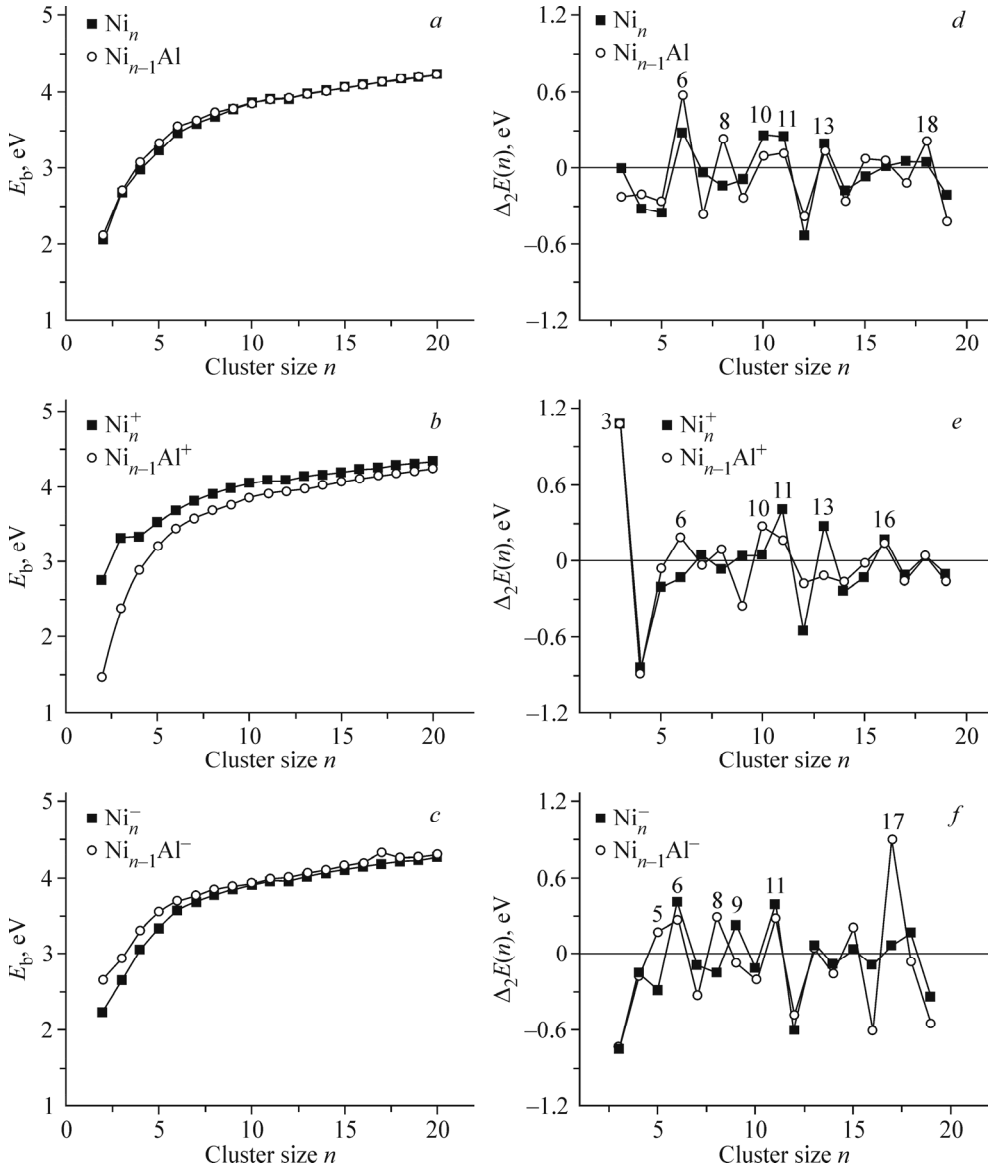

Fig. 4. Binding energy per atom of Ni_n and $Ni_{n-1}Al$ (n = 2-20) for neutral (*a*), cationic (*b*), and anionic clusters (*c*); and the second energy difference of Ni_n (n = 3-19), for neutral (*d*), cationic (*e*), and anionic clusters (*f*).

magnetic moment caused by the unpaired electron orbital motion is relatively small. The atomic total magnetic moment depends mainly on the electronic spin magnetic moment. As shown in Fig. 5*a*, the total magnetic moments obtained for $Ni_{n-1}Al$ clusters from our calculation have the same trend as pure Ni_n clusters, which increase monotonically as a function of the cluster size. The calculated total magnetic moments decrease with the addition of an Al atom, but in all these clusters the Al atom has negligible magnetic moments, which is in good agreement with previous results [5, 7, 8]. The main reason is that the relative displacement between the spin up and spin down of the cluster electron can indicate the degree of splitting. The higher the degree of spin splitting for the density of states, the stronger the spin polarization of the cluster, the greater the magnetic moment. The non-magnetic Al atom has an effect on the electron spin polarization of nickel clusters, which leads to the reduction of the total magnetic moment. In addition, we can discuss the reason for the reduction of the magnetic moment from charge transfer. Due to that the charge is transferred from the aluminum atom to nickel clusters, the charge transfer can cause a decrease in the number of unpaired 3*d* electrons and the magnetic moment is reduced. However, the total magnetic moment of $Ni_{18}Al$ is very close to Ni_{19} which has a perfect double-icosahedron structure. Their larger net spin would be related to the double-icosahedron structure.

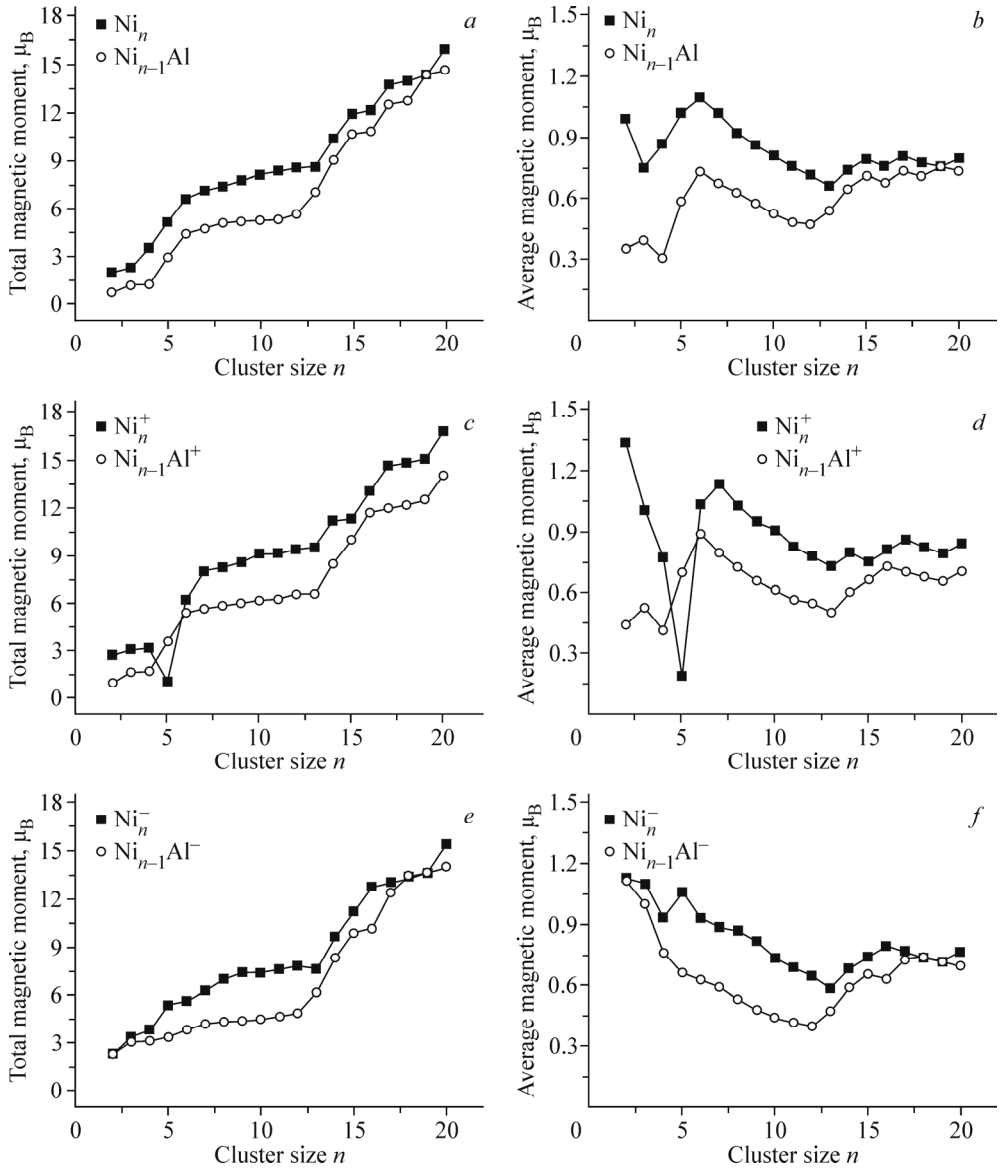

Fig. 5. The total and average magnetic moments (in μ_B units) of the Ni_n and $Ni_{n-1}Al$ (n = 2-20) clusters for neutral (*a-b*), cationic (*c-d*), and anionic clusters (*e-f*).

To further understand the impact of the cluster size on the magnetic moment, we can compare the average magnetic moment per atom of the Ni_n and $Ni_{n-1}Al$ clusters in Fig. 5*b*. As a result, it is found from observing Fig. 5*b* that the average magnetic moment per atom of the Ni_n and $Ni_{n-1}Al$ clusters exhibits an oscillating behavior. Ni_6, Ni_5Al and Ni_{13}, Ni_3Al correspond to the local maxima and minima, respectively.

Next we have also plotted the total and average magnetic moments per atom for the cationic and anionic clusters as shown in Fig. 5*c-f*, respectively. Similar to the corresponding neutral clusters, the $Ni_n^{+\backslash -}$ total magnetic moment is larger than that of $Ni_{n-1}Al^{+/-}$ except Ni_5^+ (Ni_4Al^+). The total magnetic moments of $NiAl^-$, $Ni_{17}Al^-$ and $Ni_{18}Al^-$ are very close to those of Ni_2^-, Ni_{18}^-, and Ni_{19}^-. From Fig. 5*d* and *f*, the local maxima and minima of the average magnetic moment per atom are observed at n = 7, 5 (Ni_n) and n = 6, 4 ($Ni_{n-1}Al$) for the cationic clusters, and at n = 2, 13 (Ni_n) and n = 2, 12 ($Ni_{n-1}Al$) for the anionic clusters. The results obtained in the present study help us choose magnetic materials.

Charge transfer. The charge transfer between the aluminum atom and nickel clusters for the neutral and ionic $Ni_{n-1}Al$ (n = 2-20) clusters are displayed in Fig. 6. The charge is transferred from the aluminum atom to nickel clusters due to

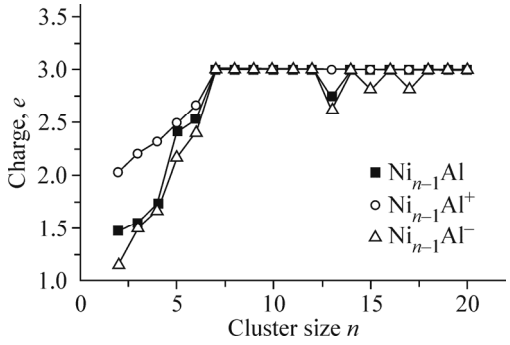

Fig. 6. Charge transfer (in e units) from the Al atom to the Ni_{n-1} (n = 2-20) clusters.

the larger nickel electronegativity (1.91) compared to that of aluminum (1.61). We found that the charge transfer amount increased as a function of the cluster size for the $Ni_{n-1}Al$ clusters. Then we have analyzed the above function based on the atomic orbital theory. The electronic configurations of Ni and Al atoms are $3d^8 4s^2$ and $3s^2 3p^1$, respectively. For the $Ni_{n-1}Al$ clusters, the Al 3*s* orbital loses electrons, the 3*p* and 3*d* orbitals obtain electrons, so the 3*s* electrons are transferred to 3*p* and 3*d* orbitals. For Ni atoms, the 4*s* electrons are transferred to 3*d* and 4*p* orbitals. Since the number of electrons that 3*d* and 4*p* orbitals obtain is less than the 4*s* orbital loses, some electrons are transferred from the Al atom to the Ni clusters. As the number of Ni atoms increases, the electrons provided by the Al atom increase gradually, too. Therefore almost all the charge is transferred from the Al atom to the Ni clusters for n = 7-20. In addition, we have also observed that the amount of the charge transfer is less for the anionic clusters than that for the neutral and cationic clusters and is especially significant for small-scale (n = 2-6) clusters. In the case of Ni_{13} and $Ni_{12}Al^{+/-}$, we noted that large charge accumulations are observed at the neighboring aluminum atom that is close to the nickel clusters, as shown in Fig. 7.

Ionization potential and electron affinity. The adiabatic ionization potential (AIP) and the adiabatic electron affinity (AEA) have been calculated based on the lowest-energy structures of the neutral and ionic Ni_n and $Ni_{n-1}Al$ (n = 2-20) clusters. AIP is the amount of energy required to remove an electron from a neutral cluster whereas AEA is the difference in the total energies of the neutral and anionic clusters. AIP and AEA are the total energy differences of the neutral and ionic clusters.

AIP is an important value in understanding the electronic properties of clusters, and it can also account for the metallicity of the clusters. Calculated AIP for the Ni_n and $Ni_{n-1}Al$ (n = 2-20) clusters are shown in Fig. 8*a*. It can be seen from the plot that AIP decreases slowly as the cluster size increases for the Ni_n clusters and exhibits an oscillating behavior for the $Ni_{n-1}Al$ clusters. AIP is larger for $Ni_{n-1}Al$ than that for the Ni_n clusters, except Ni_5 (Ni_4Al) and Ni_{17} ($Ni_{16}Al$). As is well known, when AIP gets smaller, the cluster will be closer to a metallic system; hence, the metallicity is weakened with the addition of an Al atom.

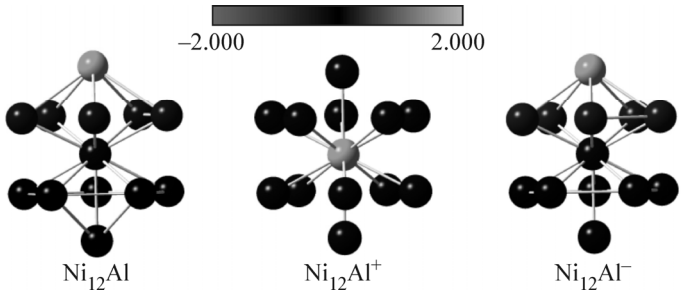

Fig. 7. Charge difference density plots of the $Ni_{12}Al$, $Ni_{12}Al^+$ and $Ni_{12}Al^-$ clusters. The gray color represents charge depletion and black color represents charge accumulation.

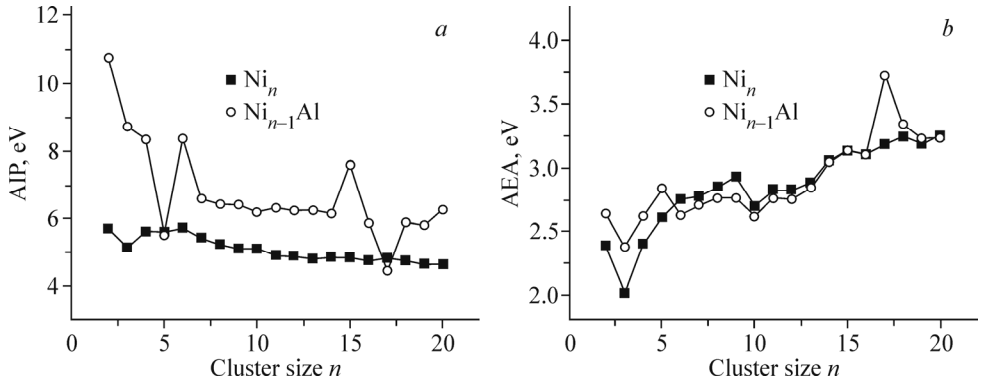

Fig. 8. AIP (*a*) and AEA (*b*) of the Ni_n and $Ni_{n-1}Al$ (n = 2-20) clusters.

AEA for the Ni_n and $Ni_{n-1}Al$ (n = 2-20) clusters have been plotted in Fig. 8*b* as a function of the cluster size. The AEA curve can be roughly divided into three regions: AEA of $Ni_{n-1}Al$ is larger for $n < 5$ and $17 < n < 19$; AEA of Ni_n is larger for $6 < n < 13$; AEA of $Ni_{n-1}Al$ is almost the same as that of Ni_n for $14 < n < 16$ and $n = 20$. Ni_3 and Ni_2Al have the lowest AEA values. Moreover, Ni_{10} and Ni_9Al show slightly smaller AEAs than their neighbors. AEA gradually increases with increasing cluster size, indicating that larger clusters capture electrons more easily. The AEA maximum is in the $Ni_{16}Al$ cluster that has the strongest ability to capture electrons.

CONCLUSIONS

In this work, we focused on analyzing a series of electronic properties of the lowest-energy $Ni_{n-1}Al$ (n = 2-20) clusters, including binding energy, magnetic property, charge transfer, ionization potential, and electron affinity, using the DFT-PBE calculations. By the analysis of the binding energy and the second energy difference of the $Ni_{n-1}Al$ clusters, we have determined the scales and structures of the relatively stable clusters, which can provide important information for the further exploration of the magic number clusters. By the analysis of the magnetic moment, we have found that the addition of the Al atom can offset some magnetic moment provided by the Ni clusters. By the analysis of the charge transfer, we have observed that the charge is transferred from the Al atom to the Ni clusters and almost all of the charges are transferred to the $Ni_{n-1}Al$ (n = 7-20) clusters. By the analysis of the ionization potential and electron affinity, we have found that the metallicity of the $Ni_{n-1}Al$ (n = 2-20) clusters is weakened by doping the Al atom. Thus, the determination of the most stable structures and the analysis of the electronic properties can help us to further understand the Ni–Al alloy clusters and provide the fundamental data for the future estimation of the magnetic materials.

This work is supported by the Natural Science Foundation of the He′nan Department of Education (grant Nos. 15B150010 and 15A140032) and the Foundation of the He′nan Educational Committee (grant No. 132300410007), and the Henan Joint Funds of the National Natural Science Foundation of China (grant No. U1404216). This work is also supported by the Xinxiang University Doctor Initial Research Program (grant Nos. 1366020018 and 1366020039) and the Science and Technology Innovation Fund of the Xinxiang University (grant Nos. 15ZP01 and 15ZB25). The computational resource is partly supported by the Performance Computing Center of the Jilin University, P. R. China.

REFERENCES

1. A. Chikhaoui, K. Haddab, S. Bouarab, and A. Vega. *J. Phys. Chem. A*, **2011**, *115*, 13997-14005.
2. Z. M. Ma and B. X. Li. *Comput. Theor. Chem.*, **2015**, *1068*, 88-96.
3. H. Q. Sun, Y. J. Bai, H. Y. Cheng, B. L. Wang, and G. H. Wang. *J. Mol. Struct.*, **2015**, *1031*, 22-29.
4. J. Q. Wen, Z. Y. Jiang, J. Q. Li, L. K. Cao, and S. Y. Chu. *Int. J. Quant. Chem.*, **2010**, *110*, 1368-1375.
5. J. Q. Wen, Z. Y. Jiang, Y. Q. Hou, and J. Q. Li. *J. Mol. Struct.* (*THEOCHEM*), **2010**, *949*, 91-95.

6. X. Zhang, B. X. Li, Z. W. Ma, and J. J. Gu. *Sci. World J*., **2013**, *468327*, 1-9.
7. M. D. Deshpande, R. Pandey, M. A. Blanco, and A. Khalkar. *J. Nanopart. Res*., **2010**, *12*, 1129-1136.
8. V. Shah and D. G. Kanhere. *Phys. Rev. B*, **2009**, *80*, 125419(1)-(8).
9. F. Y. Hao, Y. F. Zhao, X. Y. Li, and F. L. Liu. *J. Mol. Struc.* (*THEOCHEM*), **2007**, *807*, 153-158.
10. C. L. Luo. *Modell. Simul. Mater. Sci. Eng*., **2000**, *8*, 95-101.
11. Y. Xiang, D. Y. Sun, and X. G. Gong. *J. Phys*. *Chem*. *A*, **2000**, *104*, 2746-2751.
12. C. L. Luo. *New J. Phys*., **2002**, *4*, 10.1-10.8.
13. W. Song, W. C. Lu, Q. J. Zang, C. Z. Wang, and K. M. Ho. *Int*. *J*. *Quant*. *Chem*., **2012**, *112*, 1717-1724.
14. W. Song, W. C. Lu, C. Z. Wang, and K. M. Ho. *Comput*. *Theor*. *Chem*., **2011**, *978*, 41-46.
15. G. Kresse and J. Hafner. *Phys*. *Rev*. *B*, **1993**, *47*, 558-561.
16. G. Kresse and J. Furthmuller. *Phys*. *Rev*. *B*, 1996, *54*, 11169-11186.
17. J. T. Lau, A. Föhlisch, M. Martins, R. Nietubyc, M. Reif, and W. Wurth. *New J. Phys*., **2002**, *4*, 98.1-98.12.